

Ionization & Recombination



- Photoionization is often the most important process in astronomical objects. Hot stars (or the accretion of material onto compact objects, as in AGN, quasars and X-ray binary systems) emit substantial UV fluxes that ionize atoms. I.P. of H = 13.6, He = 24.6, 54.4eV.
- Photons with $E > 13.6$ eV can photoionize hydrogen the dominant gas species, though atoms with lower I.P. will be ionized with lower energy photons.



where X^i is the atom or ion that is ionized by the incident photon $h\nu$.
 X^{i+1} is the resulting ion and e^- the liberated electron

- In an idealised model HII region, the Stromgren sphere is the region within which hydrogen is ionized. It has a uniform density and a sharp boundary and may be stratified with regions of He^{++} and He^+ if the star is sufficiently hot.
- It may be surrounded by a region where H is neutral, but low I.P. species may be ionized (Mg, Na etc). Beyond that, there may be molecular gas.

Hydrogen Recombination

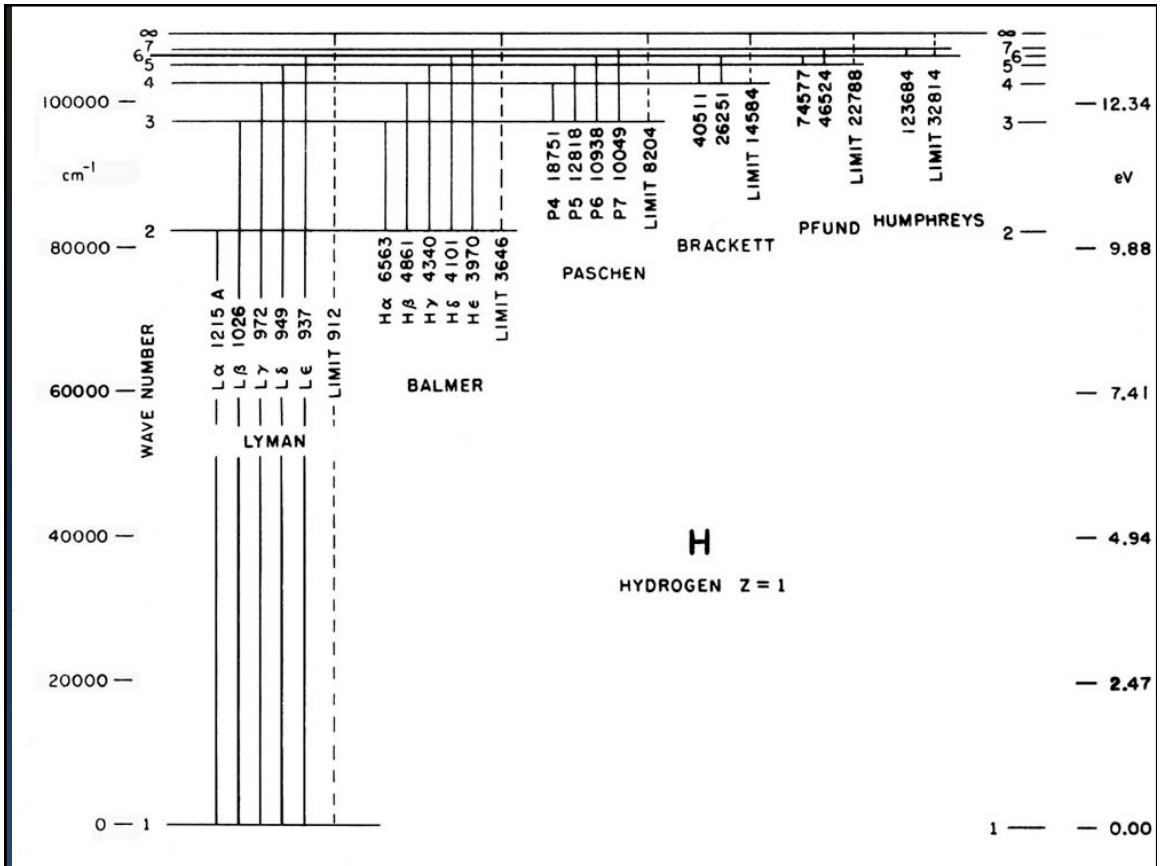
Free electrons recombine with protons into bound energy levels and rapidly cascade down to the ground state, emitting hydrogen series photons.

Transitions to the ground state ($n=1$) form the Lyman series with lines between 121.6 nm (Ly(alpha)) and the series limit at 91.2nm (which corresponds to the ionization potential of H).

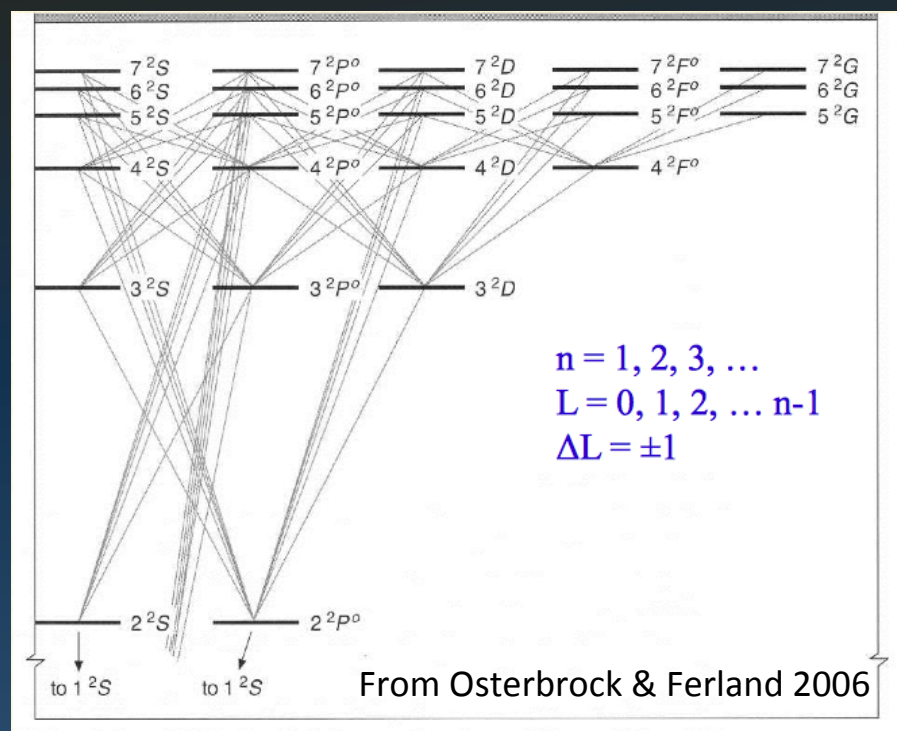
The Balmer ($n \rightarrow 2$) series lies in the visible, from H(alpha) 653 nm ($n= 3 \rightarrow 2$) to the series limit at 364 nm (corresponding to the ionization energy from $n=2$), and further series in the infrared.

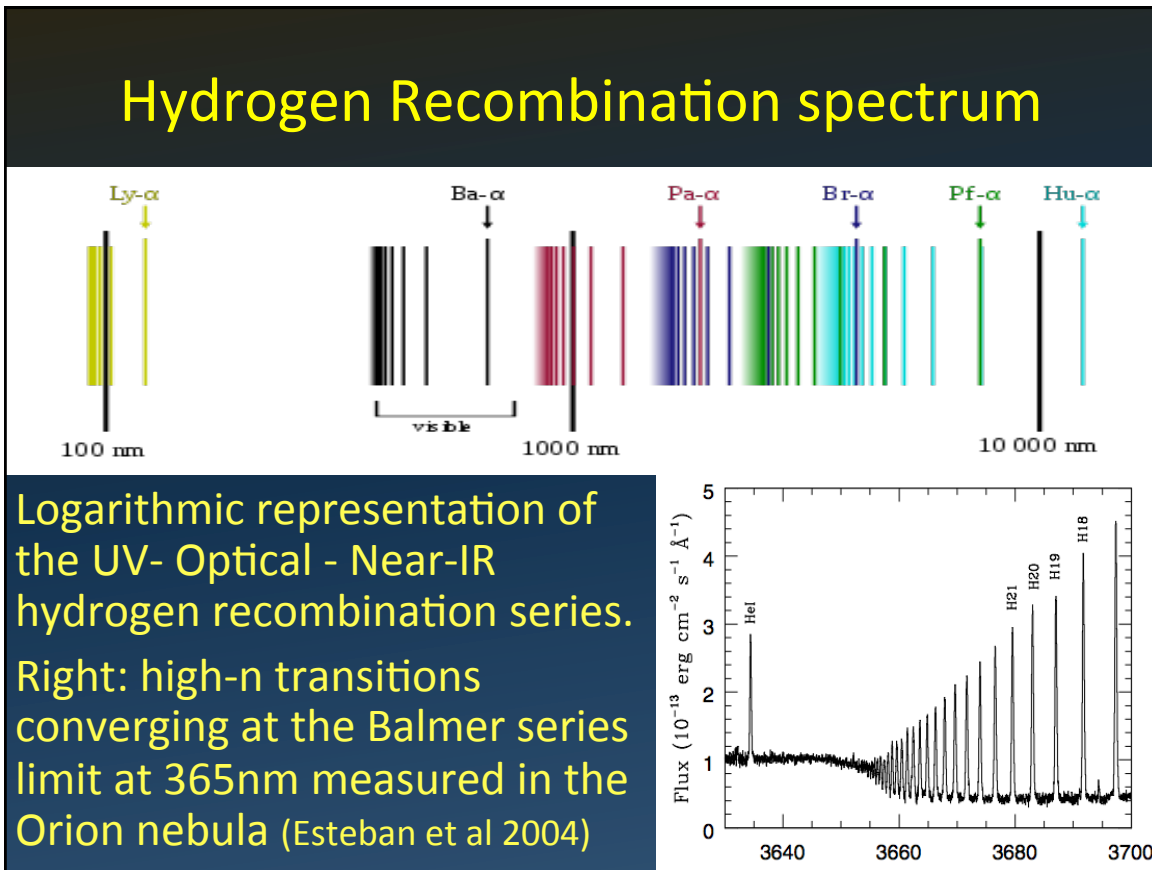
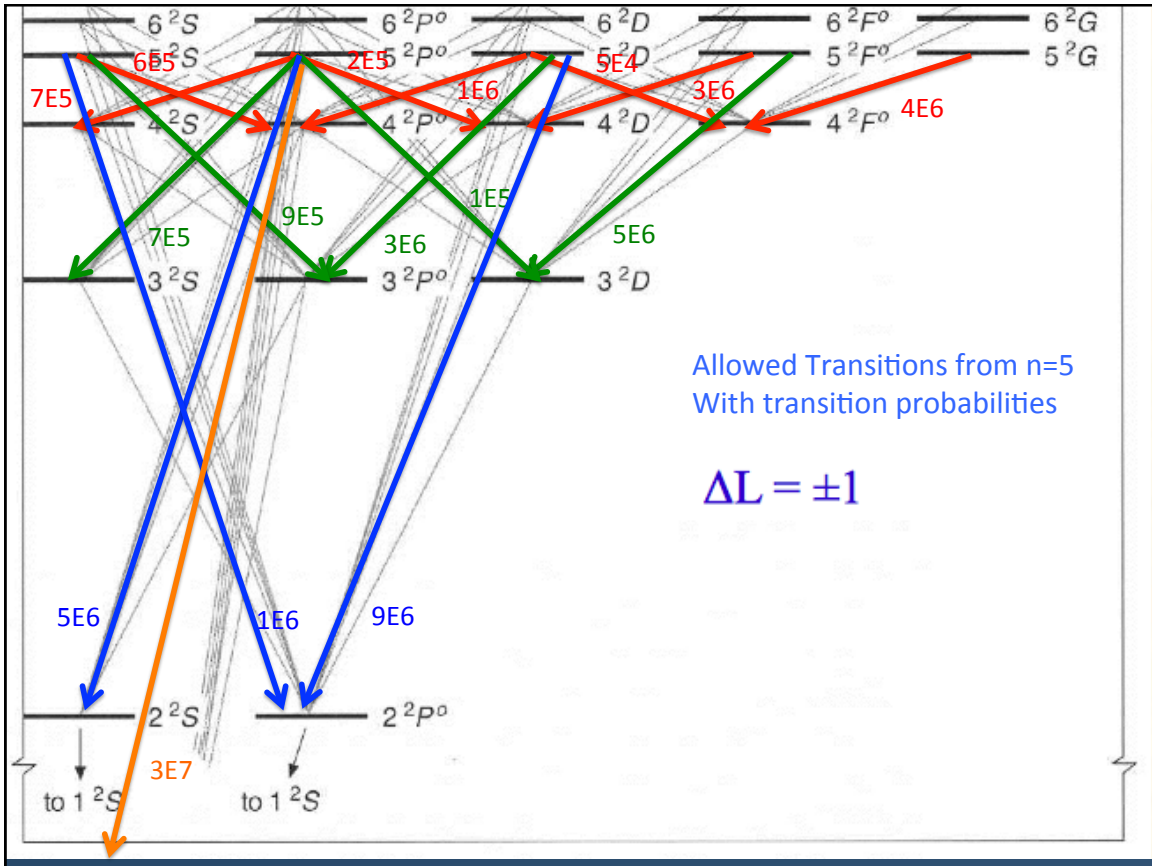
The emitted line intensities reflect the level populations through recombination and the transition probabilities down to lower levels.

Note: recombination lines are also seen from other species – especially He and He^+ but also C,N,O however the latter are usually orders of magnitude weaker, reflecting their much lower abundances.



H Recombination Transitions





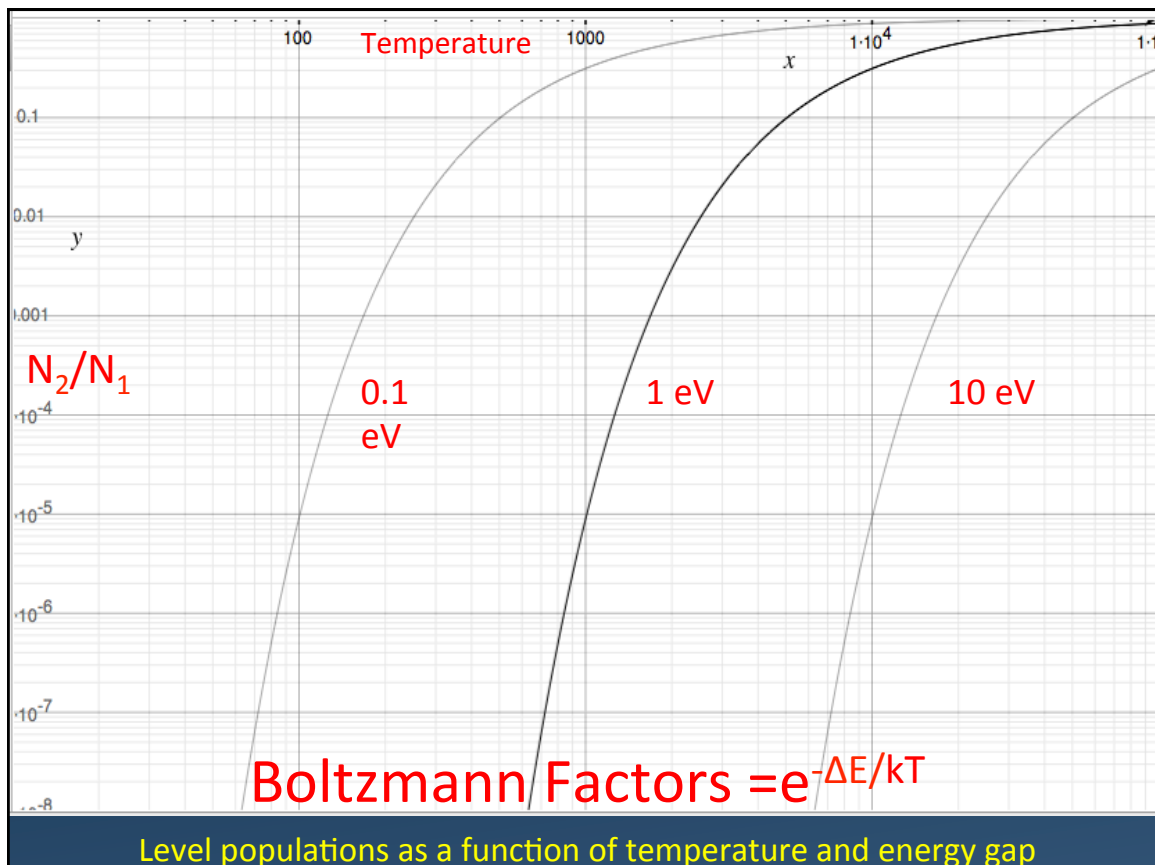
H Line spectrum

The spontaneous emission coefficients for the H lines have values $A > 10^6 \text{ s}^{-1}$, while the collisional cross sections have values $Q \sim 10^{-10} \text{ m}^3 \text{ s}^{-1}$.

This means that collisional transitions for Hydrogen are important only at densities $n_e \geq A/Q = 10^{16} \text{ m}^{-3}$.

The energy difference between the ground state and level 2 is $\sim 10 \text{ eV}$. At nebular temperatures, $\Delta E < kT_e$ and collisional excitation is unimportant at T_e below 10^4 K .

Below these values of T_e and n_e , the level population are determined primarily by the A values, and so are only weakly dependent upon N_e and T_e .



Absorption probabilities

The ionization cross section (for photons at 912 Å) is $\sigma_{v_0} = 6.30 \times 10^{-18} \text{ cm}^2$. This is orders of magnitude smaller than the absorption cross sections of the low-n Lyman lines. So the bright Lyman lines are absorbed by nearby atoms, producing enormous optical depths, and maintaining high ionization fractions. The mean free path $\sim 1/(\sigma_{v_0} n_H) \sim 2 \cdot 10^5 \text{ pc}$ or 1 A.U. for $n_H \sim 10^4 \text{ cm}^{-3}$

Line	Wavelength (Å)	A (sec ⁻¹)	a ₀ (cm ²)	$\tau_0/\tau_{912 \text{ Å}}$
Ly α	1215.67	6.26×10^8	5.90×10^{-14}	9366
Ly β	1025.72	1.67×10^8	9.46×10^{-15}	1501
Ly γ	972.54	6.82×10^7	3.29×10^{-15}	522
Ly 10	920.96	4.21×10^6	1.72×10^{-16}	27
Ly 15	915.82	1.24×10^6	5.00×10^{-17}	8
Ly 20	914.04	5.24×10^5	2.10×10^{-17}	3

Recombination Coefficients

Calculated by integrating the probability of e- capture by a proton and branching ratios into all levels. Definitive tables by Hummer & Storey (MNRAS 224, 801. 1987). These give the recombination coefficient as a function of density and temperature and the line intensities that result, relative to Hβ (n=4-2): $\alpha_B = 2.6 \times 10^{-13} \text{ cm}^3 \text{ s}^{-1}$

H TE = 1.00+04 NE = 1.00+04 CASE B NC = 70

TOTAL RC = 2.592-13 4-2 RC = 3.034-14 4-2 EM = 1.240-25 2S RC = 8.422-14 2P RC = 1.750-13

NU	NL	2	3	4	5	6	7	8	9	10	11	12	13	14	15
50	8.39-04	2.58-04	1.11-04	5.75-05	3.36-05	2.13-05	1.43-05	1.01-05	7.39-06	5.57-06	4.30-06	3.39-06	2.72-06	2.21-06	2.21-06
45	1.08-03	3.31-04	1.43-04	7.40-05	4.32-05	2.74-05	1.85-05	1.30-05	9.54-06	7.19-06	5.56-06	4.38-06	3.51-06	2.86-06	2.86-06
40	1.43-03	4.40-04	1.90-04	9.87-05	5.78-05	3.67-05	2.48-05	1.75-05	1.28-05	9.66-06	7.47-06	5.89-06	4.73-06	3.85-06	3.85-06
35	1.99-03	6.16-04	2.67-04	1.39-04	8.19-05	5.22-05	3.53-05	2.50-05	1.83-05	1.38-05	1.07-05	8.47-06	6.80-06	5.55-06	5.55-06
30	2.90-03	9.08-04	3.98-04	2.10-04	1.24-04	7.99-05	5.43-05	3.87-05	2.85-05	2.16-05	1.68-05	1.33-05	1.07-05	8.75-06	8.75-06
29	3.15-03	9.87-04	4.35-04	2.30-04	1.37-04	8.78-05	5.99-05	4.27-05	3.15-05	2.39-05	1.86-05	1.47-05	1.19-05	9.71-06	9.71-06
28	3.41-03	1.08-03	4.75-04	2.52-04	1.50-04	9.70-05	6.63-05	4.73-05	3.50-05	2.66-05	2.07-05	1.64-05	1.32-05	1.08-05	1.08-05
27	3.71-03	1.17-03	5.22-04	2.78-04	1.66-04	1.08-04	7.37-05	5.27-05	3.90-05	2.97-05	2.31-05	1.84-05	1.48-05	1.21-05	1.21-05
26	4.05-03	1.29-03	5.75-04	3.08-04	1.85-04	1.20-04	8.24-05	5.90-05	4.38-05	3.34-05	2.60-05	2.07-05	1.67-05	1.37-05	1.37-05
25	4.43-03	1.42-03	6.36-04	3.43-04	2.07-04	1.34-04	9.26-05	6.65-05	4.94-05	3.77-05	2.94-05	2.34-05	1.89-05	1.55-05	1.55-05
24	4.87-03	1.56-03	7.07-04	3.83-04	2.32-04	1.52-04	1.05-04	7.53-05	5.60-05	4.28-05	3.34-05	2.66-05	2.15-05	1.76-05	1.76-05
23	5.37-03	1.74-03	7.91-04	4.31-04	2.62-04	1.72-04	1.19-04	8.59-05	6.40-05	4.90-05	3.83-05	3.05-05	2.46-05	2.01-05	2.01-05
22	5.97-03	1.94-03	8.91-04	4.89-04	2.99-04	1.97-04	1.36-04	9.86-05	7.36-05	5.63-05	4.41-05	3.51-05	2.83-05	2.32-05	2.32-05
21	6.68-03	2.18-03	1.01-03	5.58-04	3.43-04	2.26-04	1.58-04	1.14-04	8.52-05	6.53-05	5.10-05	4.06-05	3.28-05	2.68-05	2.68-05
20	7.54-03	2.47-03	1.16-03	6.43-04	3.97-04	2.63-04	1.83-04	1.33-04	9.94-05	7.61-05	5.95-05	4.73-05	3.81-05	3.10-05	3.10-05
19	8.58-03	2.83-03	1.33-03	7.47-04	4.63-04	3.08-04	2.15-04	1.56-04	1.17-04	8.94-05	6.99-05	5.54-05	4.45-05	3.61-05	3.61-05
18	9.87-03	3.28-03	1.56-03	8.77-04	5.46-04	3.64-04	2.54-04	1.85-04	1.38-04	1.06-04	8.25-05	6.53-05	5.22-05	4.20-05	4.20-05
17	1.15-02	3.84-03	1.84-03	1.04-03	6.50-04	4.34-04	3.04-04	2.21-04	1.65-04	1.26-04	9.81-05	7.73-05	6.13-05	4.83-05	4.83-05
16	1.35-02	4.56-03	2.20-03	1.25-03	7.82-04	5.23-04	3.66-04	2.66-04	1.99-04	1.52-04	1.17-04	9.17-05	7.13-05	5.28-05	5.28-05
15	1.62-02	5.49-03	2.66-03	1.52-03	9.53-04	6.38-04	4.47-04	3.24-04	2.42-04	1.84-04	1.41-04	1.08-04	8.42-05	6.53-05	6.53-05
14	1.97-02	6.72-03	3.27-03	1.87-03	1.18-03	7.88-04	5.52-04	4.00-04	2.97-04	2.24-04	1.68-04	1.21-04	9.17-05	7.13-05	7.13-05
13	2.44-02	8.37-03	4.09-03	2.35-03	1.48-03	9.89-04	6.92-04	5.00-04	3.68-04	2.72-04	1.92-04	1.41-04	1.08-04	8.42-05	8.42-05
12	3.09-02	1.06-02	5.21-03	2.99-03	1.89-03	1.26-03	8.82-04	6.32-04	4.57-04	3.17-04	2.24-04	1.68-04	1.21-04	9.17-05	9.17-05
11	4.00-02	1.38-02	6.79-03	3.91-03	2.46-03	1.65-03	1.14-03	8.04-04	5.45-04	3.90-04	2.83-04	2.07-04	1.52-04	1.14-04	1.14-04
10	5.33-02	1.84-02	9.09-03	5.24-03	3.30-03	2.20-03	1.50-03	9.90-04	6.92-04	5.00-04	3.68-04	2.72-04	1.92-04	1.41-04	1.41-04
9	7.34-02	2.54-02	1.26-02	7.25-03	4.56-03	2.99-03	1.91-03	1.31-03	9.40-04	6.88-04	5.00-04	3.68-04	2.72-04	1.92-04	1.92-04
8	1.05-01	3.65-02	1.81-02	1.04-02	6.49-03	4.01-03	2.71-03	1.91-03	1.31-03	9.40-04	6.88-04	5.00-04	3.68-04	2.72-04	2.72-04
7	1.59-01	5.53-02	2.75-02	1.58-02	9.27-03	5.76-03	3.84-03	2.59-03	1.81-03	1.31-03	9.40-04	6.88-04	5.00-04	3.68-04	3.68-04
6	2.60-01	9.01-02	4.47-02	2.45-02	1.58-02	9.27-03	5.76-03	3.84-03	2.59-03	1.81-03	1.31-03	9.40-04	6.88-04	5.00-04	5.00-04
5	4.69-01	1.62-01	7.77-02	4.47-02	2.45-02	1.58-02	9.27-03	5.76-03	3.84-03	2.59-03	1.81-03	1.31-03	9.40-04	6.88-04	6.88-04
4	1.00+00	3.32-01	1.62-01	7.77-02	4.47-02	2.45-02	1.58-02	9.27-03	5.76-03	3.84-03	2.59-03	1.81-03	1.31-03	9.40-04	9.40-04
3	2.85+00	1.62-01	7.77-02	4.47-02	2.45-02	1.58-02	9.27-03	5.76-03	3.84-03	2.59-03	1.81-03	1.31-03	9.40-04	6.88-04	6.88-04

Dependence of H line ratios on T_e

$$\frac{F(\text{H}\alpha)}{F(\text{H}\beta)} = 2.86 \left(\frac{T_e}{10^4 \text{ K}} \right)^{-0.07}$$

$$\frac{F(\text{Br}\alpha)}{F(\text{H}\beta)} = 0.079 \left(\frac{T_e}{10^4 \text{ K}} \right)^{-0.36}$$

$$\frac{F(\text{Br}\gamma)}{F(\text{H}\beta)} = 0.028 \left(\frac{T_e}{10^4 \text{ K}} \right)^{-0.24}.$$

These approximations hold to 1% over the range :

$100 < n_e < 10000 \text{ cm}^{-3}$ and $5000 < T_e < 12000 \text{ K}$ and so are valid for many nebulae.

The ratio of ionizing photons to the number of $\text{H}\alpha$ photons = 2.2 within these ranges, and so measurement of the Balmer lines gives a good estimate of N_i providing that the Ly series is optically thick and the Balmer lines are optically thin. This condition is known as Menzel's Case B. In this case, all of the Lyman lines are multiply scattered in the nebula and only emerge as transitions to level 2 (Balmer series) or higher.

Metal lines arise from trace elements and are usually optically thin

Line Emission

Recombination coefficients are calculated from the photoionization cross sections and summed for recombination to all atomic levels.

The total recombination coefficient should be used in the low density limit, Case A, which occurs where the Lyman lines are optically thin.

The intensity of emission lines can be expressed in terms of the effective line emissivity j_ν – usually given for $\text{H}\beta$.

In thermal equilibrium, $j_\nu = \kappa_\nu B_\nu(T)$, but the recombination process produces level populations that are far from LTE.

In case B, the $\text{H}\beta$ emission line luminosity :

$$L_{\text{H}\beta} = \int 4\pi n_e n_p j_\nu dV$$

where $j_\nu(T)$ is the line emissivity of $\text{H}\beta$.

$$j_\nu(T) = N_p N_e \alpha hc / (4\pi\lambda) \text{ Wm}^{-3}$$

Continuum Emission

In addition to emission lines, the electrons in the ionized gas give rise to free-free and free-bound transitions

Free-free emission is usually most important at radio wavelengths where the Rayleigh Jeans approximation can be used for thermal emission.

The electrons have a thermal Maxwellian distribution at $T_e \sim 10^4$ K. At long wavelengths, we can use the Rayleigh-Jeans approximation:

as $j_\nu = k_\nu B_\nu(T)$

$$B_\nu(T) = \frac{2kT}{\lambda^2} = \frac{j_\nu}{k_\nu}$$

$$k_\nu \propto T_e^{-1.5} \nu^{-2.1} \int n_e n_p ds$$

The opacity :

$$\tau_\nu = \int k_\nu ds \propto \int \frac{n_e n_p}{\nu^{2.1} T^{3/2}} ds$$

and the optical depth :

Free-free

Now

$$\tau_\nu = \int \frac{n_e^2}{\nu^{2.1} T^{3/2}} ds$$

At high radio frequencies $\tau \ll 1$ and so the flux S_ν is:

$$S_\nu \propto \frac{2kT\nu^2}{c^2} \tau_\nu \propto \nu^{-0.1}$$

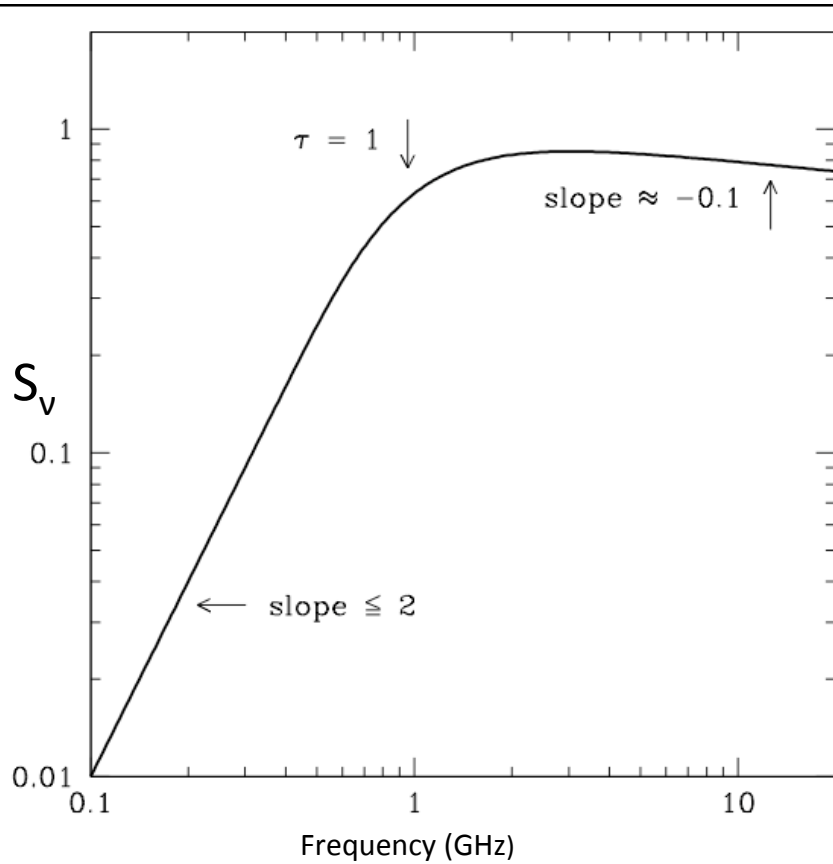
As the frequency decreases, the opacity increases until it becomes optically thick and the flux then falls with decreasing frequency as a R-J BB tail, ν^2 , with a turnover at $\tau=1$.

Note: the quantity $\int n_e n_p dV$ is known as the emission measure (for a pure hydrogen nebula)

Representative free-free spectrum
 Plotted as S_ν against ν as usual at radio frequencies.

The optical depth increases with decreasing frequency until the emission becomes optically thick, when it follows a Rayleigh Jeans blackbody slope.

At higher frequencies thermal dust emission usually becomes dominant



Stromgren Sphere

- The extent of the Stromgren sphere is determined by the ionization and recombination of H atoms. i.e. the flux of ionizing photons with $E > 13.6\text{eV}$
- A hot star emits N_i ionizing photons per second, and we assume that all of these are eventually absorbed by H atoms in the surrounding HII region. In equilibrium, the rate of recombinations equals N_i .
- With a radiative recombination coefficient α , the recombination rate per unit volume per second:

$$N_r = \alpha n_e n_H$$

- For a fully ionized, pure hydrogen nebula, $n_e = n_H$, and within the volume V the radius of the Stromgren sphere is:

$$r_s^3 = \frac{3N_i}{4\pi\alpha n_H^2}$$

- This is an idealised model HII region, but gives an estimate of the size of an HII region around a particular star surrounded by a region of a certain density.

- The H_β line flux from an idealised sphere

$$F_{H_\beta} = \frac{4\pi r_s^3}{3} \frac{4\pi j_\nu}{4\pi D^2}$$

Stromgren Sphere in more detail

- In equilibrium, the recombination rate equals N_i . Because radiative transitions have very short lifetimes, excited states will rapidly decay to the ground state, so we can treat all H atoms as being in the ground state.
- The photoionization rate from the ground state is balanced by the total recombination rate to all levels in the H atom.

$$n_{1s} \int_{\nu_1}^{\infty} \frac{4\pi J_{\nu}}{h\nu} a_{\nu}(1s) d\nu = \alpha_A(T_e) n_e n_p$$

- However a recombination directly to the ground state emits a Lyman continuum photon which immediately is absorbed in ionizing another nearby H atom so we actually use the recombination coefficient to just the excited states (i.e. excluding to the ground state) α_B

At $T=10^4\text{K}$, $\alpha_B = 2.6 \times 10^{-19} \text{ m}^3 \text{ s}^{-1}$

$$r_s^3 = \frac{3N_i}{4\pi\alpha_B n_H^2}$$

Resulting HII region

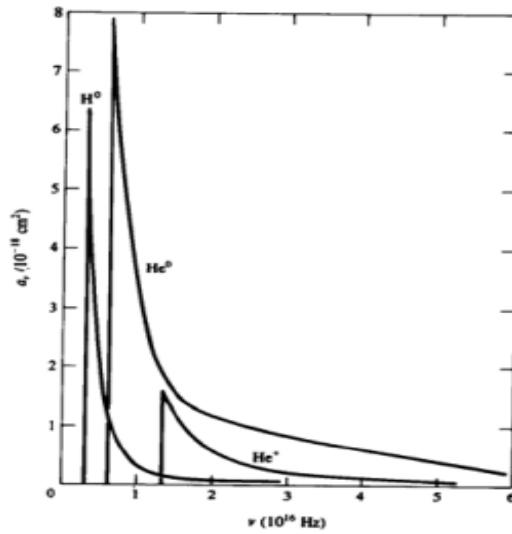
- With a recombination coefficient, $\alpha = 2.6 \times 10^{-19} \text{ m}^3 \text{ s}^{-1}$ (appropriate for $T_e \sim 10^4 \text{ K}$), we can estimate the radius of the Stromgren sphere around different types of star. Adopting a density of 10^{10} m^{-3} .

Sp Type	$N_i (\text{s}^{-1})$	$r_s (\text{pc})$
G2V	10^{39}	6.7E-5
B0V	4×10^{46}	1.6E-2
O6V	10^{49}	0.1

Note that the HII region can be either matter bounded or radiation bounded, where the Stromgren sphere extends beyond the surrounding material or is contained within it.

A similar calculation can be carried out for He (IP = 24.6eV)

Figure 4.3 Photoionization absorption cross section of H⁰, He⁰, and He⁺.



The photo-ionization (bound-free) cross sections increase abruptly from zero at the IP and are high at energies just above that energy, falling as ν^{-3} .

Note that $\sigma(\text{He I}) > \sigma(\text{H})$ above the IP(He I). Figure from Osterbrock for H I, He I and He II.

$$\sigma_{\nu}^{\text{bf}} \approx \left(\frac{1}{4\pi\epsilon_0} \right)^5 \frac{64\pi^4 Z^4 m_e e^{10}}{3^{3/2} c h^6 \nu^3 n^5} \approx 2.81 \times 10^{25} \frac{Z^4}{\nu^3 n^5} \text{ m}^2$$

He and H photoionization model

Note the large difference in the extent of the He ionization zone

(from Osterbrock)

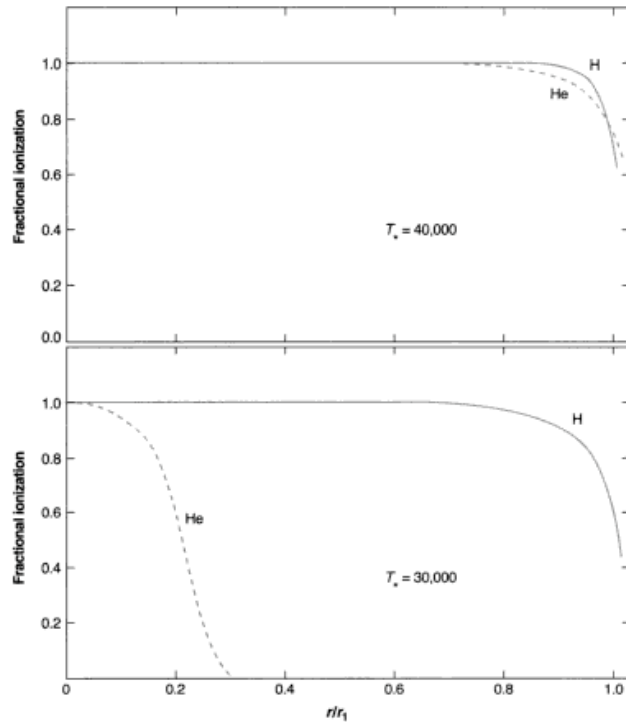


Figure 2.4 Ionization structure of two homogeneous H⁺ He model H II regions.

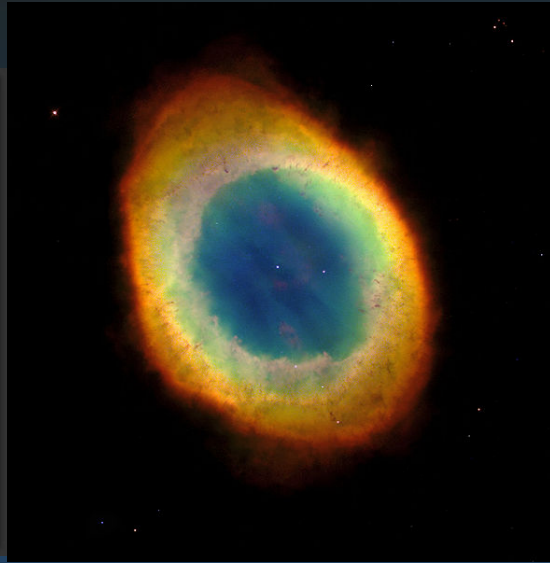
The Rosette nebula



© Anglo-Australian Obs./Royal Obs. Edinburgh

A young HII region almost 1 deg across illuminated by a cluster of OB stars (NGC 2244) which have cleared out a central cavity

M57 The Ring Nebula



Planetary nebula showing stratification

Red [NII] 6584
Green [OIII] 5007
Blue Helium 4686



The Orion nebula seen with HST. The dominant ionizing source is θ^1 Ori, of spectral type O6, but there are thousands of newly formed stars in the central parsecs

Recombination and Ionization Timescales

The recombination coefficient, $\alpha_B = 2.6 \times 10^{-19} \text{ m}^3 \text{ s}^{-1}$, which with a density of 10^{10} m^{-3} gives a recombination time of $\sim 3 \times 10^8 \text{ s} \sim 10 \text{ yr}$.

The total recombination rate over the volume of the HII region is:

$$R = \frac{4\pi}{3} r^3 n_e \alpha_B n_p$$

As a hot star forms, it will start to ionize its surroundings and the ionization front will advance through the surrounding medium. The timescale for advance depends on the density of the medium and N_i .

The number of H atoms in a shell outside an ionized sphere is

$$4\pi r^2 n_H(r) \Delta r$$

while the number of ionizing photons available in time Δt is $N_i \Delta t$, and the number of ionizing photons available for ionizing the shell is the total number - the number of recombinations within the ionized zone

$$4\pi r^2 n_H(r) \Delta r = N_i \Delta t - \frac{4\pi}{3} r^3 n_e \alpha_B n_p \Delta t$$

With $n_e = n_p = n_H$:

$$4\pi r^2 n_H(r) \frac{dr}{dt} = N_i - \frac{4\pi}{3} r^3 \alpha n_H^2(r)$$

The expression for the Stromgren radius:

$$r^3 = r_s^3 = \frac{3N_i}{4\pi\alpha n_H^2}$$

Now define $\tau = t/\tau_{\text{rec}}$ where $\tau_{\text{rec}} = 1/\alpha n_H$, and $\lambda = r/r_s$, to express the equations in terms of the recombination time and Stromgren radius,

to give:

$$4\pi\lambda^2 n_H(r) \frac{r_s^3}{\tau_{\text{rec}}} \frac{d\lambda}{d\tau} = N_i - \frac{4\pi}{3} r_s^3 \lambda^3 \alpha n_H^2(r)$$

And multiplying by τ_{rec}/r_s^3 :

$$4\pi\lambda^2 n_H(r) \frac{d\lambda}{d\tau} = N_i \frac{\tau_{\text{rec}}}{r_s^3} - \frac{4\pi}{3} \lambda^3 n_H(r)$$

Now

$$\frac{N_i \tau_{\text{rec}}}{r_s^3} = \frac{4\pi n_H}{3} \Rightarrow 3\lambda^2 \frac{d\lambda}{d\tau} = 1 - \lambda^3$$

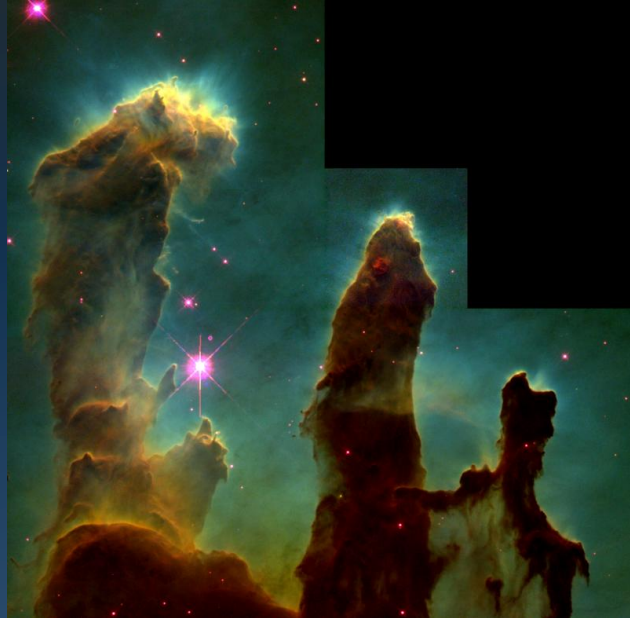
And for uniform density, the solution is

$$\lambda^3 = 1 - \exp(-\tau) \Rightarrow r(t) = r_s [1 - \exp(-t/t_{\text{rec}})]^{1/3}$$

The 'Pillars of Creation' or The Eagle Nebula or M 16

As an ionization front advances through a cloud, residual dense structures remain after photoevaporation of lower density material

Dense cores are the sites of star formation and so newly formed stars may lie in the cores of dense globules



Estimates of stellar temperature

The ionizing photons produce H emission lines (and an associated free-free continuum) in well-understood flux ratios, with a relatively weak dependence on temperature and density.

This holds for the normal range of nebular conditions, but at high densities, collisional effects become important.

The Ly continuum flux increases sharply from stars of type B0 to O4 (Mass ~ 10 to $40M_{\odot}$), rising as $\sim T^7$. Measurement of H lines allows us to infer the number of ionizing photons in a nebula.

If the total luminosity can be measured (integrated over the whole spectrum), then the ratio of the energy in ionizing photons compared to L_{bol} gives an estimate of the effective temperature of the exciting star(s).

In practice, some Ly α photons do escape from the nebula (multiple scattering means that some have wavelengths that random walk to the edge of the line profile so that the cross section decreases).

Stellar Models

The number of high energy photons (producing highly ionized species such as He²⁺) depends on the detailed shape of the stellar spectrum which is complex and poorly understood for many objects.

Getting accurate estimates of the effective temperature of the exciting stars requires careful comparison between observations and models

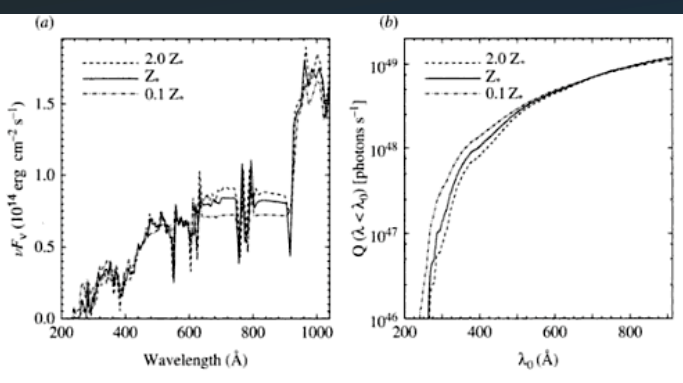


Figure 7.17 (a) Non-LTE unified photosphere/wind (CMFGEN) model for an O6 dwarf ($T_{\text{eff}} = 41\,010$, $\log g = 4.014$, $L = 2.54 \times 10^3 L_{\odot}$) for three different metallicities. All spectra have a strong metal-line forest contributing to the absorption, in particular below 700 \AA . To bring out the overall effect of these line forests the spectra have been re-binned. The prominent features around 550 and 600 and between 700 and 800 \AA are blends of wind lines from different ionization stages of carbon, nitrogen, oxygen, and silicon. (b) The cumulative photon luminosity for wavelengths smaller than λ_0 as a function of λ_0 . Figure adapted from R. Mokiem, *et al.*, 2004, *A. & A.*, **419**, p. 319.

The effects of Dust

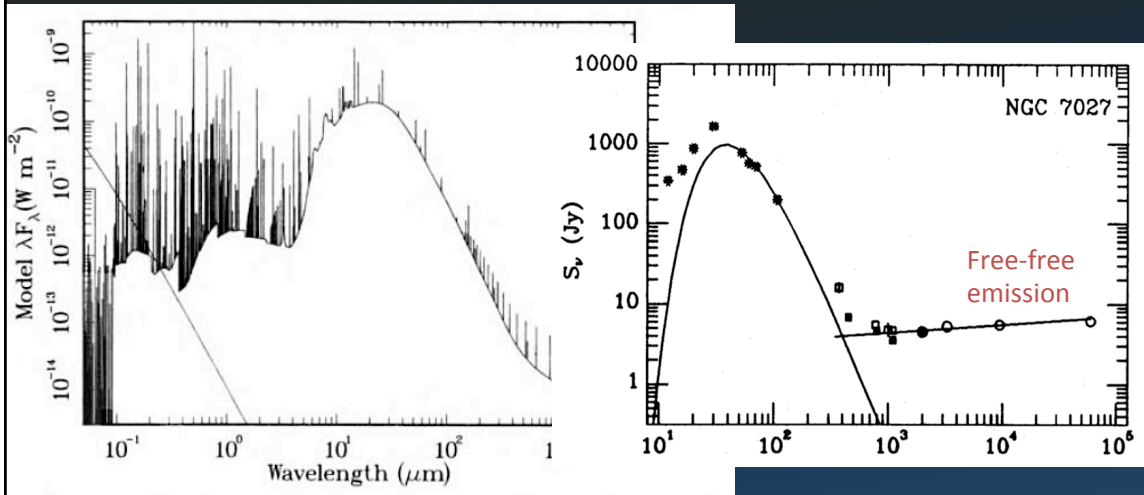


Fig. 6.2. The model spectrum of NGC 7027 from UV to radio. the thin (almost straight) line on the left is the continuum (226,000 K blackbody) of the central star.

In the idealised HII region we have assumed that all Lyman photons are trapped and multiply scattered, populating electrons in excited levels until they emit in the Balmer or higher series .

However, if dust is mixed with the gas, some fraction of the photons will be absorbed by dust grains. The grains are heated and will emit thermal infrared photons, but this then means that N_{H} will be underestimated.

In this PN, dust absorbs most of the UV photons, and most of the luminosity emerges in the IR.

Collisional Ionization

- Is important in hot plasmas with densities substantially higher than in typical nebulae
- Here an electron is scattered as it passes an ion, giving up sufficient energy to remove a bound e^-



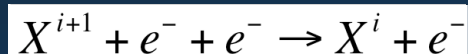
- The collisional ionization rate coefficient Q_i is obtained by integrating $q v f(v)$ where q is the ionization cross-section and $f(v)$ is usually assumed to be Maxwellian, so that $Q_i = \bar{q}v$
- The ionization rate per unit volume is then $Q_i N_i N_e$ (s^{-1}) and Q_i can be approximated as:

$$Q_i = 2 \times 10^{14} \frac{\xi}{\chi^2} T_e^{1/2} e^{-\chi/kT_e} \quad m^3 s^{-1}$$

- Where ξ is the number of electrons in the subshell .
- Collisional ionization may be important when kT_e is larger than the hydrogen ionization potential, χ , i.e. at $T > 20,000K$.

Collisional Recombination

- Collisional recombination is the inverse of collisional ionization, but note that it requires a 3 particle interaction between two free electrons and an ion.



- This will only be important in regions of very high density such as stellar interiors and need not be considered in nebulae

Collisional excitation and autoionization

In ions that have more electrons in an inner subshell than in an outer shell, excitation of an inner electron is quite likely.

E.g. in a configuration such as $2p^63s$, an inner electron may be excited to a higher level giving $2p^53snl$ (e.g. Na I, Mg II, Al III ... Fe XVI)

The excited state produced can lie above the ionization potential of the ion (the energy required to remove the outermost electron – $3s$ in this example).

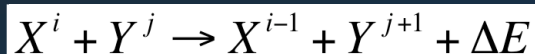
Consider Fe XVI ground state $2s^22p^63s$ Na I – like ion

Collisional excitation of a p shell electron gives an excited state $2s^22p^53snl$ which lies above the ground state of Fe XVII $2s^22p^6$

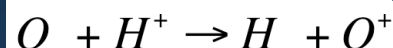
The excited state can either decay spontaneously back to the ground state, emitting an EUV photon, or make a radiationless transition into the continuum (analogous to Auger transitions from inner shells). In this case, the electron becomes unbound and results in ionization to Fe XVII

Charge Exchange

- Charge exchange occurs when an electron is exchanged between an atom and an ion.
- Here X and Y are an atom and ion of different elements.



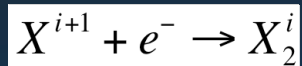
- Charge exchange is most important when the energy difference ΔE is small, and where the probability of exchange is high
- The ionization potentials of H and O are 13.598 and 13.618 eV respectively i.e. $\Delta E = 0.02\text{eV}$



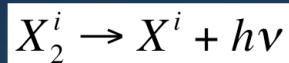
- The reverse process is important at the edge of HII regions where the H^+ fraction decreases and because of the large number of neutral H atoms, O becomes predominantly neutral. Charge exchange is the most important recombination process from O II to O I
- Because of the small O abundance, this process does not alter the H ionization structure of the HII region

Di-electronic recombination

- Dielectronic recombination occurs when an ion in the ground state has an electron excited by a passing electron, which is itself captured forming a doubly excited state X_2 in ion X^i .



- This excited state may be above the first ionization state of X^i and can decay by autoionization, producing X^{i+1} or it can decay to a lower level in ion X^i , emitting a photon and constituting a recombination.



- This process is important in hot plasmas at moderate densities (e.g. in the solar corona) and in low ionization stages at nebular temperatures (e.g. for Planetary Nebulae)

Excitation and Recombination Processes

- Different processes dominate under different conditions, and so in order to know which approach to take, we need to be able to estimate the prevailing density and temperature in the medium under study.
- We can do this by using pairs of transitions that are sensitive to the density, e.g. because they have very different collisional rates, and so the ratio of the line intensities varies as a function of the density.
- Most diagnostic measurements use lines in the optical because they have well proven and are well understood, but as spectra in other wavelength regimes have become more sensitive, diagnostics in e.g. the infrared are becoming more important, and benefit from reduced sensitivity to the effects of interstellar reddening